HHS Public Access

Author manuscript

J Biomed Mater Res B Appl Biomater. Author manuscript; available in PMC 2018 February 01.

Published in final edited form as:

J Biomed Mater Res B Appl Biomater. 2017 February ; 105(2): 366–375. doi:10.1002/jbm.b.33561.

Bone Regeneration in Critical Bone Defects Using Three-Dimensionally Printed β-Tricalcium Phosphate/Hydroxyapatite Scaffolds Is Enhanced by Coating Scaffolds with Either Dipyridamole or BMP-2

Stephanie Ishack[1], **Aranzazu Mediero**[2], **Tuere Wilder**[2], **John L. Ricci**[1], and **Bruce N. Cronstein**[1]

[1] Department of Biomaterials and Biomimetics NYU College of Dentistry, New York, NY, USA

[2] Division of Translational Medicine, Department of Medicine, NYU-Langone Medical Center. New York, NY, USA

Abstract

Bone defects resulting from trauma or infection need timely and effective treatments to restore damaged bone. Using specialized three-dimensional (3-D) printing technology we have created custom 3-D scaffolds of hydroxyapatite (HA)/Beta-Tri-Calcium Phosphate (β-TCP) to promote bone repair. To further enhance bone regeneration we have coated the scaffolds with dipyridamole, an agent that increases local adenosine levels by blocking cellular uptake of adenosine. 15% HA: 85% β-TCP scaffolds were designed using Robocad software, fabricated using a 3-D Robocasting system, and sintered at 1100°C for 4h. Scaffolds were coated with BMP-2 (200ng/ml), Dypiridamole 100μM or saline and implanted in C57B6 and adenosine A2A receptor knockout (A2AKO) mice with 3mm cranial critical bone defects for 2-8 weeks. Dipyridamole release from scaffold was assayed spectrophotometrically. MicroCT and histological analysis were performed. micro-computed tomography (microCT) showed significant bone formation and remodeling in HA/β-TCP- dipyridamole and HA/β-TCP -BMP-2 scaffolds when compared to scaffolds immersed in vehicle at 2, 4 and 8 weeks (n=5 per group; $p \leq 0.05$, $p \leq 0.05$ and $p \leq 0.01$, respectively). Histological analysis showed increased bone formation and a trend toward increased remodeling in HA/β-TCP- dipyridamole and HA/β-TCP-BMP-2 scaffolds. coating scaffolds with dipyridamole did not enhance bone regeneration in A2AKO mice. In conclusion, scaffolds printed with HA/β-TCP promote bone regeneration in critical bone defects and coating these scaffolds with agents that stimulate A2A receptors and growth factors can further enhance bone

Corresponding author: Bruce N. Cronstein, MD, Division of Translational Medicine, Department of Medicine, New York University School of Medicine, 550 First Avenue, MSB251, New York, NY 10016., Bruce.Cronstein@nyumc.org., Phone number: 1-212-263-2978, Fax number: 1-646-501-6840.

Disclosures:

A.M. and B.N.C. have filed a patent on use of adenosine $A_{2A}R$ agonists to prevent prosthesis loosening (Patent number 8183225). A.M., B.N.C have filled a patent on use of anti-netrin-1 antibodies for the treatment of bone disease (pending). AM.M. S.I. J.R. and B.N.C. had filled a papent about the use of tissue repair devices and scaffolds. B.N.C. holds patents numbers 5,932,558; 6,020,321; 6,555,545; 7,795,427; adenosine A_1R and $A_{2B}R$ antagonists to treat fatty liver (pending); B.N.C. is a consultant for Bristol-Myers Squibb, Novartis, CanFite Biopharmaceuticals, Cypress Laboratories, Regeneron (Westat, DSMB), Endocyte, Protalex, Allos, Inc., Savient, Gismo Therapeutics, Antares Pharmaceutical, Medivector, King Pharmaceutical, Celizome, Tap Pharmaceuticals, Prometheus Laboratories, Sepracor, Amgen, Combinatorx, Kyowa Hakka, Hoffman-LaRoche and Avidimer Therapeutics. BNC has stock in CanFite Biopharmaceuticals.

regeneration. These coated scaffolds may be very useful for treating critical bone defects due to trauma, infection or other causes.

Keywords

3-D-printing; scaffold; bone defects; dipyridamole; hydroxyapatite (HA)/Beta-Tri-Calcium Phosphate (β-TCP)

Introduction

Over 2 million long bone fractures are treated in the United States every year [1]. Although most bone fractures heal spontaneously in pathological fractures or large and massive bone defects, bone healing and repair fail, and bone autografts are generally used to promote healing [2]. The materials used in bone grafting can be divided into several major categories, including autografts, allografts, and xenografts; autografts remain the ‘gold standard’ in reconstructing small bone defects and have strong osteogenic characteristics relevant to bone healing, modeling, and remodeling [3] The regeneration and repair of bone requires a source of mesenchymal stem cells that can differentiate into bone-forming osteoblasts.. Like autografts, bioresorbable scaffolds can direct the migration of these stem cells into the defected area and can promote the formation of a vascular network capable of supporting the bone. Thus, when autografts are not practical bioresorbable scaffolds can be used to enhance bone regeneration [4].

Combined or not with various carriers or scaffolds, growth factors such as bone morphogenetic proteins (BMPs), mesenchymal stem cells, and a variety of other agents have been used to promote repair of bone defects. To date, an optimal approach has not been clearly demonstrated. We have recently demonstrated that adenosine and an agent that stimulates an increase in extracellular adenosine, dipyridamole, promote bone growth via interaction with specific adenosine A2A receptors on bone cells [5].

Adenosine, a purine nucleoside produced in the extracellular fluid by the hydrolysis of adenine nucleotides, can bind to and stimulate specific receptors (A1, A2A, A2B and A3) present on the surface of most cells. These receptors are members of the large G protein coupled receptor family which signals for cellular functions, in general, via either inhibition or stimulation of cAMP accumulation [6]. In recent studies we have reported that adenosine A2A receptors (A2ARs), which are expressed on osteoclast and osteoblast precursors as well as endothelial cells, regulate both bone metabolism and angiogenesis *in vitro* and *in vivo* [7-12]. Moreover, A2AR stimulation inhibits bone destruction by diminishing inflammation, decreasing osteoclast number and function and increasing osteoblast number and bone formation at sites of inflammatory bone destruction [7-12]. Moreover, results of our recent studies demonstrate that ligation of A2AR by a specific agonist or by treatment with dipyridamole, an agent that increases local adenosine concentrations by blocking cellular adenosine uptake, increases bone regeneration in murine calvarial defects [5].

Significant interest has been devoted to the utilization of bioactive ceramic materials in the repair and regeneration of extensive long bone defects. The driving force for calcium-

phosphate-based bioactive ceramic development arises not only from their well-established osteoconductive properties but also from the often encountered, limited autogenous bone available for placement in or around defects, and the associated difficulty in obtaining uneventful healing with seamless integration between grafted and native bone [13-15]. However, limitations in the degradation kinetics and mechanical properties of synthetic bioactive ceramics have hampered their use due to unpredictable replacement of the synthetic material by bone and mechanical integrity of the ceramics over time. We have recently integrated materials engineering, manufacturing, and bone healing expertise to develop three-dimensional (3-D) structures that present adequate degradation kinetics for long bone healing purposes, are mechanically robust for surgical placement, osteoconductive, and customizable to each individual's needs regarding long-bone segmental defect regeneration [16]. The 3-D printing technology is widely spreading in the healthcare field. Based on imaging techniques (microCT and magnetic resonance imaging (MRI)), the 3-D images of the bones can be re-constructed, and based on the symmetry of the human anatomy, the software used can mimic the 3-D images of the bones at the missing parts, therefore customized manufacture bone prostheses can be implanted into human body [17, 18]. The optimal scaffold for bone repair/replacement should be readily available, closely fit the damaged bone area, prevent infection, provide mechanical stability, recruit cells to the site for repair, promote fast bone growth into the scaffold, and eventually remodel leaving normal bone behind. Using specialized three-dimensional (3-D) printing technology we can design custom scaffolds for bone repair composed of materials with these optimal characteristics and combine them with coatings and fillers that can provide improved healing of critical bone lesions. Direct-write (DW) fabrication allows for 3-D creation of off the shelf or custom parts with tailored interconnected porosity that other methods lack. Thus, we have developed hydroxyapatite (HA)/Beta-Tri-Calcium Phosphate (β-TCP) printable scaffold components that provide mechanical strength, conduct bone throughout the scaffold and remodel over time [16, 19-21]. Moreover, coating these porous scaffolds with osteoinductive agents such as BMP-2 can further stimulate bone growth over the scaffold [19].

Because use of bone morphogenetic proteins, such as BMP-2, may cause both local complications and even distant cancers [22, 23], finding other osteoinductive agents that can be used to promote bone growth in association with printed scaffolds presents a challenge. To further optimize the capacity of bioresorbable ceramic scaffolds to promote closure of critical bone defects we have combined the osteoinductive qualities of adenosine receptor stimulation with the osteoconductive qualities of printed calcium triphosphate/ hydroxyapatite ceramic scaffolds to promote more rapid bone ingrowth into calcium triphosphate/hydroxyapatite scaffolds. We report here evidence that coating ceramic scaffolds with dipyridamole promotes bone ingrowth on ceramic scaffolds via ligation of adenosine A2A receptors and that dipyridamole promotes bone growth as well as BMP-2.

Materials and Methods

Assembly of HA and βTCP scaffolds

The robocasting of 15% HA:85% β-TCP composite scaffold assembly is a multistep process involving ink preparation, printing, sintering, and filling [24-26]. The ink for the scaffolds was fabricated through a series of powder processing steps, beginning with calcination (800°C for 11 hrs), attrition milling (3 mm zirconia milling media; Union Process, Akron, OH) in DI-H2O for approximately 30 minutes, and drying (~65-75°C) of the beta-tricalcium phosphate (β-TCP), Sigma-Aldrich, Germany). The dried ceramic was then transferred into a polyethylene bottle and dry milled for ~10 minutes utilizing a paint shaker with a charge of ~ 20 pieces of zirconia milling media of 10mm diameter (D) [26]. The previously calcined and milled ceramic powders were used for the colloidal gel formulation. Concentrated β-TCP suspensions, where volume fraction ($\phi_{ceramics}$) of ceramic was $\phi_{ceramics}$= ~0.46, were produced by mixing a pre-calculated amount of ceramic powder and ammonium polyacrylate (Darvan 821A; RT Vanderbilt, Norwalk, CT) solution to disperse particles into DI-H_2O. The dispersant proportion per gram of ceramics was ~15 mg. First, about 25 g of milling media was added to the DI-H_2O, then the dispersant, and then the ceramic powder in 3 parts (~33% per step). After each addition of powder, the suspension is mixed in the planetary mixer (Thinky AR-250; Thinky, Tokyo, Japan) for 1 minute. Next, hydroxypropylmethylcellulose, also referred to as F4M, (Methocel F4M; Dow Chemical Company, Midland, MI) was added as the thickening agent. The F4M is used in a 5% by weight aqueous solution with a proportion of 7 mg per milliliter of ceramic. The suspension was then mixed for 1 minute followed by a defoaming step for 1 minute in the planetary mixer. Finally, the suspension was gelled by adding ~150 mg per 30 mL of ink of polyethyleneimine (PEI) (Sigma-Aldrich, St. Louis, MO) 10% by weight solution. Mixing and defoaming (1 minute and 30 seconds, respectively) after the final addition completed the ink preparation procedure [19, 26] .

The β-TCP scaffolds were fabricated via robocasting, utilizing a 3-D direct-write microprinter gantry robot system to extrude the colloidal ink (Aerotech Inc. Pittsburgh, PA). The scaffolds were constructed layer-by-layer using a 3-axis motion control robot, which can extrude the HA and β-TCP inks at a constant volumetric flow rate through standard syringe needles. Custom CAD software controls the position of the deposition nozzle and the rate at which the plunger pushes material through the syringe. The 3-D circular ‘plug’ shaped scaffolds with cap (cap layer diameter 4.4-mm, ‘plug’ diameter 3.3-mm, 250-μm struts, and 300-μm pore spacing) were designed utilizing a computer-aided design (CAD) system (RoboCAD 4.1; 3D Inks LLC Tulsa, OK) (Figure 1). The colloidal ink was loaded into a 3-ml syringe (EFD Inc., Nordson, Westlake, OH) and subsequently equipped with 250-μm-diameter extrusion nozzle (EFD Inc., Nordson, Westlake, OH). The 3-D circular ‘plug’ shaped scaffolds were printed in layer-by-layer fashion at 8 mm/s print speed. The entire deposition process occurred in a low-viscosity paraffin oil tray to prevent drying of the structure during fabrication. After the scaffold was complete, it was removed from the oil reservoir and allowed to partially dry, The scaffolds were then fired in a furnace (Model LH3 02/17, Nabertherm, Germany). The firing sequence included a slow ramp heating at 2°C/minute until 400°C, stationary at 400°C for 1 hour, then higher speed heating till 900°C

(8.3°C/min.), stationary for 2 hours at 900°C, heating 3.3°C/min. to 1100°C, then a plateau at 1100°C for 4 hours, and finally a rapid cooling at 9.1°C/minute until the samples achieve room temperature. The design of the scaffold is shown in Figure 1. The optimal composition of the ink used for the printed scaffolds (15:85 HA/βTCP) was previously determined and is described [26].

Formulation of depot forms of dipyridamole on ceramic and collagen-coated ceramic scaffolds for use in the promotion of bone regeneration

To prepare collagen coated scaffolds, 8 parts of bovine collagen type I solution (BD Biosciences, Franklin Lakes, NJ, USA) were mixed with 1 part of 0.01M NaOH, and 1 part of PBS10X and pH was adjust at 7.4±0.2, all done at 4 C. Scaffolds were cover with this collagen solution, incubate 20 minutes at 37 C and collagen crosslinking was performed by irradiation (120uW/cm^2 for 15 minutes). The uncoated or coated scaffolds were then immersed in a solution of dipyridamole (100μM) (Sigma-Aldrich, St. Louis, MO, USA), and placed in 0.5 ml saline at 37 C for up to 10 days (n=5 each). The kinetics of dipyridamole release was tested after 0, 0.3, 0.5, 1, 12, 24, 48, 72, 96, 120 and 240 hours of immersion in saline (n=5 each time point) and was detected as absorbance$_{405nm}$.

Implantation of scaffolds into trephination wounds in murine skulls

The NYUSoM Institutional Animal Care and Use Committee approved all protocols related to animals. C57Bl/6 and adenosine A2A knockout (KO) mice (on a C57Bl/6 background (>10 backcrosses)) were anesthetized by intraperitoneal injection of ketamine and xylazine. The hair over the skull was shaved and the underlying skin was aseptically prepared. A full thickness midline incision, extending from the nasofrontal to occipital region, was made under sterile conditions. The subcutaneous tissue was sharply dissected along the same line as the skin. The underlying periosteum was sharply incised on the midline and subsequently elevated off the skull to obtain sufficient exposure for the trephine. A full thickness 3 mm defect was created to remove bone from the middle of the dorsal calvarium was accomplished using a biopsy pounch (Acu Punch, Acuderm Inc., Ft. Lauderdale, FL, USA) with caution to prevent damage to the underlying sagittal sinus and dura matter. A bioresorbable digitally printed collagen-coated Calcium triphosphate/hydroxyapatite matrix soak in saline or dipyridamole 100μM (soaking time of about 5 minutes) was then applied to the 3 mm diameter calvarial defect (n=5 each treatment). Following the procedure mice were injected with Lidocaine 0.5% subcutaneously at the operative site, no further analgesics were administered. Skin in all the animals was closed with 4-0 nylon and sutures were removed in 7-10 days. In some animals collagen coated scaffolds were immersed in a solution containing BMP-2 (200ng/ml), or CGS21680 (a selective adenosine A2A agonist) 100μM (n=5 each) (soaking time of 5 minutes). Water and food were given ad libitum until sacrifice. Animals were sacrificed after 2, 4 and 8 weeks of defect formation in a CO_2 chamber and the calvaria were removed, fixed, and prepared for micro-computed tomography (microCT) and histological staining.

Implant preparation for analysis

Specimens were removed with surrounding bone with a scalpel at 2, 4 and 8 weeks. Specimens were stored in 70% ethanol and coarsely dehydrated in series of graded alcohols.

The specimens were then embedded in polymethyl methacrylate according to standard hard tissue histology protocols described by Bromage [27]. Briefly, after dehydration, specimens were immersed in Methyl Salicylate for 30 hours, with a change in solution after 6 hours. Tissue was infiltrated with Methyl Methacrylate, changing the solution every 24 hours 3 times to ensure complete infiltration (first infiltration at room temperature and the other two at 4ºC). After this, solution was changed again and samples were kept under uv light until polymerization. The specimen was trimmed of excess polymer and sectioned.

Micro-computed tomography (microCT) analysis

Specimens were examined by micro CT (CT40- Scanco Medical, Basserdorf, Switzerland). Micro-CT of all scaffolds was carried out at medium resolution, integration time 300 ms with 30.7 holder size and average data of 2. The resulting voxel was 14.8 um and the field of view was 15.2. The initial microCT data collection was performed at 50 kVp, 200 μA with a resolution of 36 μm. Three hundred slices were taken with 15μm y angle, which results in scanning of a 1500μm thickness portion of the scaffold. These slices were then chosen in the middle of the scaffold that is surrounded by bone. Four empty scaffolds were analyzed by Micro-CT to give preliminary measurement of scaffold volume, empty space volume, thickness of struts and pore sizes. Empty scaffolds were analyzed the same way the implanted scaffolds were analyzed. This group was considered as a zero time point group in order to compare to the other groups. As the HA/β-TCP ink in this study was resorbable, some areas had similar density to bone especially at the edges of the struts; peripheral areas of the scaffolds were not included. The identical volume and site of the scaffold was measured in order to get a “standard” measurement. For quantitative analysis of new bone formation, an area of interest was segmented manually by marking the volume of interest (VOI) a round-shaped region across the bone defect of approximately 3 mm. The threshold was adjusted until different structures could be distinguished i.e. separating bone from scaffold. A threshold of 352–1982 mg HA/cm^3 for bone was determined by using the empty HA-BTCP scaffold as a standard. Within VOI, scaffold volume was determined and measured and then soft tissue volume was measured. To differentiate between scaffold and bone, the density threshold for an unimplanted β-TCP scaffold was determined at 639–1982 mg HA/cm^3; this value was subsequently used in the assessment of the implanted β-TCP scaffolds. Tissue within a threshold of 352–639 mg HA/cm^3 was considered as remodeled bone. Bone volume was determined by subtraction of the summation of scaffold volume and soft tissue volume fraction from one (Bone fraction = 1 – (Soft tissue fraction+ scaffold fraction). Marrow spaces were counted as soft tissue. Scaffold was analyzed in total and then analyzed in different quadrants separately..

Histological analysis

Blocks were cut in coronal section and ground down manually to the chosen section level on one side using a series of graded emery papers to 1200 grit (Buehler, IL, USA). With the ground face down, the embedded specimen was placed onto the slide with thin film of glue (Gorilla Super Glue, Cincinnati, Ohio, Gorilla Glue, Inc). The block was then sectioned and the finish polished to ≈100μm thickness. Coronal plane sections were stained with Van Gieson's picrofuchsin and Stevenel Blue to determine tissue response. In this procedure,

calcified bone stains bright red with an intensity that varies according to bone maturity. Cells, fibers and unmineralized matrix stains blue, and scaffold is unstained.

Histomorphological analysis

Digital photographs of the sections were scanned by Aperio microscope (SCANSCOPE GL, CA, USA), then displayed on the computer for analysis. Pictures were displayed by Image Scope viewer which imports single high-quality, ultra-resolution digital scans that multiple magnified images could be selected from. In this case the original magnification was 20x (0.5 microns/pixel for 20x). Using standard histological techniques, cell types and morphologies were determined in higher magnification. Using the same digital photographs, percentage of bone surface area in the region of interest was calculated. Thresholding of bone, scaffold and soft tissue based on the colors of the histology image were segmented by Photoshop (version 7) program. Scaffold was manually colored by blue, bone by pink and soft tissue by green. The percentage of each structure in the colored picture was calculated by Leica program (Leica QWin, Wetzlar, Germany).

Statistical Analysis

In these experiments there were 5 mice in each group for microCT, histologic and immunohistologic experiments. The effects of time and treatment of each group were tested by two-way ANOVA using a Bonferroni test as a non-parametric post-hoc test. One-way ANOVA with Bonferroni testing as a non-parametric post-hoc test was used to compare the mean of each treatment at each specific time point

Results

Dipyridamole is released from scaffolds

In our initial studies we determined the optimal method for coating ceramic scaffolds with dipyridamole following immersion in a solution of dipyridamole (100μM). We compared coating scaffolds with bovine collagen to no coating and observed that the kinetics of dipyridamole release by the scaffolds into the supernatant media was consistently higher in the scaffolds coated with bovine collagen (0.002±0.0003 mM vs 0.0013±0.00005 mM, $p<0.001$, n=5) (Figure 2). Because dipyridamole concentrations greater than 1μM are required to achieve optimal effects on bone regeneration [28] *in vivo* we found that immersing scaffolds in solutions containing concentrations of dipyridamole of 1μM or 10μM did not consistently achieve adequate concentrations of dipyridamole in the supernate (data not shown).

Blockade of adenosine uptake by dipyridamole increases bone regeneration *in vivo*

We next compared bone regeneration on bovine collagen-coated scaffolds implanted into a calvarial defect following scaffold immersion in saline, BMP-2 or a solution of dipyridamole. Analysis of microCT images of the implanted scaffolds demonstrated that there was significantly more bone growth into dipyridamole- or BMP-2-coated scaffolds than control scaffolds by 2 weeks after implantation (29.6±6% for dipyridamole and 33.9±3% for BMP-2 vs 12.8±2% for control, $p<0.001$) and this increase persisted throughout all of the time points tested (32.7±6% for dipyridamole and 39.2±10% for

BMP-2 vs 16.4±2% for control at 4 weeks, 47.5±5% for dipyridamole and 48.3±4% for BMP-2 vs 34.1±5% for control at 8 weeks, $p<0.001$ respectively) (Figure 3). Interestingly, there was widespread bone growth over the inside of the calvaria distant from the BMP-2-coated scaffolds whereas bone growth was almost completely confined to the scaffolds in the control and dipyridamole-treated scaffolds (Figure 3). This widespread bony outgrowth is consistent with clinical reports of exuberant ectopic bone formation following the use of BMP-2 as an adjunct in the surgical treatment of the spine [29].

Histologic examination of implanted scaffolds demonstrates a marked increase in bone ingrowth into the BMP-2 and dipyridamole-coated scaffolds over control scaffolds. Quantitation of bone ingrowth by histomorphometric examination of scaffolds confirms that bone ingrowth into dipyridamole- and BMP-2-coated scaffolds was greater than into control scaffolds (47.9±3% for dipyridamole and 48.2±5 for BMP-2 vs 31.2±5 for control at 8 weeks, $p<0.001$) (Figure 4). Moreover, the magnitude of the difference in bony ingrowth, determined histolomorphometrically, between the dipyridamole- and BMP2-coated scaffolds was similar to that observed by quantitation of bone ingrowth by microCT.

To determine whether the osteoinductive effects of dipyridamole-coated scaffolds were mediated by enhanced adenosine release and ligation of adenosine A2A receptors we implanted control, BMP-2-, CGS21680- (a selective adenosine A2A agonist) or dipyridamole-coated scaffolds into adenosine A2A receptor-deficient mice and studied bony ingrowth (microCT) over 4 weeks. We found that the effects of BMP-2 on bone growth were similar in the A2A receptor-deficient mice to those observed in wild type mice but that the effects of dipyridamole-coating were completely abrogated in the A2A receptor-deficient mice, similar to the effect shown for CGS21680, consistent with the prior results [5] indicating that dipyridamole indirectly stimulated A2A receptors by increasing local adenosine concentration at the site of application (21±3% for dipyridamole, 20±4% for CGS21680 and 27±5% for BMP-2 vs 20±3% for control at 4 weeks, p=ns, p=ns, $p<0.01$ respectively) (Figure 5).

Discussion

Previously we have demonstrated that inhibition of osteoclast formation via A2AR stimulation or increasing local adenosine concentration, via blockade of adenosine uptake by ENT1 with dipyridamole, stimulates new bone formation as well as rhBMP-2, a growth factor currently marketed for promotion of bone growth [5]. Nonetheless, our approach of daily administration of dipyridamole to a collagen sponge was not the most efficient approach to mirror BMP-2 effects in bone regeneration and a scaffold with better mechanical properties (to maintain proper bridging of the bone defect and for minimal weight bearing) capable of sustained release of the compound is essential, more importantly, to be useful in the clinic. Therefore, we have combined the capacity of bioresorbable ceramic scaffolds to promote closure of critical bone defects with the osteoinductive qualities of dipyridamole. We report here that resorbable printed 15% HA:85% β-TCP scaffolds can be used to fill in critical bone defects and provide a template on which bone can form. Moreover, we found that coating these osteoconductive scaffolds with

dipyridamole provides sustained release of the osteoinductive agent (Figure 2) and enhances bone growth over the scaffold as well as BMP-2.

Dipyridamole has been used systemically (both orally and intravascularly in patients) for decades with little evidence of systemic toxicity; and the occurrence of severe drug-related adverse effects, including cardiac death or cerebral ischemic attack is less than 0.02% of patients taking systemic doses of the agent [30, 31]. Therefore, dipyridamole is a safe drug that could be used safely to promote bone formation and will not have the same spectrum of local or systemic side effects observed when BMP-2 has been used for promotion of bone regeneration.

Implantation of BMP2-coated scaffolds led to nearly as much new bone formation over uninvolved calvaria at sites distant from the scaffold as there was over the surface of the scaffold. BMP2 has been used to promote bone growth in patients following spinal surgery and bone overgrowth and ectopic bone formation are well described complications of the use of BMP2 [29, 32], as we noted here. In contrast, there was very little or no ectopic bone growth distant from the dipyridamole-coated scaffolds. This difference in ectopic bone formation is most likely due to levels of dipyridamole that were ineffective at promoting bone growth at sites distant from the scaffold.

We have previously reported that dipyridamole and selective adenosine A2A receptor agonists promote regeneration in a murine trephine defect and, as seen in these studies, the increase in bone regeneration was not apparent in mice lacking adenosine A2A receptors. The dipyridamole-induced increase in bone regeneration is mediated by both suppression of osteoclast differentiation and function and by an increase in osteoblast-mediated bone formation [5]. We have clearly demonstrated that A2A receptor stimulation diminishes osteoclast differentiation and function in a manner consistent with A2A receptor-mediated inhibition of NFκB signaling [5, 9, 11, 33]. In contrast, A2A receptor stimulation does not alter osteoblast differentiation although it clearly regulates osteoblast expression of proteins involved in bone formation [5, 33]. The studies on A2A receptor responses described above were carried out with cells from bone removed at the time of prosthetic implant (most likely femur or tibia) and the absence of A2A receptors led to changes in bone density in long bones due to altered bone formation and remodeling. Thus, although the type of bone in the calvaria differs from that in long bones and the behavior of the cells in bone responsible for these effects may also differ between the calvaria and long bones it is likely that the calvarial model used provides at least suggestive evidence that the dipyridamole-coated scaffolds will be effective in the treatment of critical bone defects in long bones as well. Moreover, the availability of A2A receptor deficient mice makes it possible to better define the pharmacology of bone regeneration in this model. Nonetheless, further studies in long bones in large animals will need to be carried out in order to demonstrate the relevance of the studies carried out in a calvarial model to the effects on critical bone defects in long bones in animals or, ultimately, in patients.

Recent studies by Tenhiusen and colleagues have provided evidence collagen itself provides a scaffold that promotes bone ingrowth with little evidence of adverse responses [34]. Moreover, live cell attachment is significantly greater on scaffolds coated with 2.5% and 5%

collagen, compared to that with 0% collagen, indicating that collagen-containing scaffolds may present a better surface for osteoconduction relative to synthetic polymers or inorganic scaffolds for tissue engineering [35]. In our study we observed that scaffolds coated with collagen had better drug delivery kinetics compared to uncoated scaffolds (Figure 2) and therefore tested the effects of dipyridamole only in collagen-coated scaffolds with collagen-coated controls. The results of these previously published studies suggest if other synthetic polymers provide better release kinetics for dipyridamole they should also be tested alone for their capacity to stimulate or inhibit bone regeneration.

The similarity of synthetic HA to bone mineral has led to the extensive use of HA as a bone grafting material in hard tissue implants. Pure HA has osteoconductive properties and the ability to support the growth of bone over the implant surface [36]. Nonetheless, concerns have been raised regarding the limited degradation properties of this material, including the slow resorption rate [26, 37]. Therefore, combination of HA with different calcium phosphate compositions have been used to improve HA properties for implantation to promote bone regeneration. Here we have used a composition of 15% HA:85% β-TCP, a bioactive composition which possess two of the ideal characteristics for grafting procedures: osteoconduction and osseointegration. Mixtures of HA and β-TCP ceramic powders have been used to provide better control of degradation/dissolution rate[26]. We did not determine the resorption rate of the scaffolds used here although there was no significant difference apparent in the rate of absorption of the scaffolds, whether coated with vehicle, BMP-2 or dipyridamole, over the time we observed these implants. When combined with medical imaging, 3-D printing has the potential to revolutionize the concept of personalized medicine. As mentioned above, medical images can be used to guide 3-D printing of products, such as customized dental fillings and fittings, designed to fit neurosurgical cranial plugs, personalized prostheses replacing generic parts, and the production of anatomically accurate models for planning operations [18]. As previously described, 3-D printing can be integrated with tissue engineering and regenerative medicine as well [38]. We designed our scaffold to maximize surface area while providing complete filling of the bone defect, and combination with the active molecule dipyridamole, fulfills the requirements for regenerative medicine described for 3-D printing-technology. It is possible that other scaffold designs might have promoted bone regeneration better. Recently is has been described that the use of 3-D printing of composite calcium phosphate scaffolds at low temperature that are promising as they allow to include the biological compound into the printing process [39-42]. In addition, low temperature 3-D printing provides the potential to create composites with synthetic or biological polymers such as collagen [41]. However, to remain biologically active, printed drugs must be resilient to the printing process [42], and therefore they must be resistant to heat as loss of biological activity is likely a result of the heat developed during thermal purging through the narrow print heads. As dipyridamole's melting point is 165-166° Celsius, this improved technique should be considered as well. Nonetheless, we envision design of scaffolds for critical bone defects on a custom basis making use of currently available imaging to aid in the design of the scaffolds. Thus, each custom-designed scaffold can be generated, coated and sterilized and shipped in on a custom basis.

In the current and previous study [5] in which the effects of dipyridamole were tested on bone regeneration the bone defects were large by murine standards but very small by human standards (3mm in diameter). Dipyridamole promoted greater bone growth in these defects when injected daily into a collagen sponge than when released from the scaffolds described here although it is unlikely that the mechanical properties of collagen sponges are appropriate for promoting bone growth in larger critical bone defects, such as may occur in a patient. Thus, it is likely that scaffolds with appropriate mechanical properties will be deployed to promote bone growth across critical defects and enhancing bone growth on these scaffolds with dipyridamole or other agents will provide added benefit.

In summary, we have described an easily customizable system for promoting bone regeneration in critical bone defects. Both the osteoconductive scaffold and the osteoinductive coating contribute to the successful efforts to promote bone regeneration in a critical bone defect.

Acknowledgements

This work was supported by grants from the National Institutes of Health (AR56672, AR54897, AR046121, RC1HL100815), the NYU-HHC Clinical and Translational Science Institute (UL1TR000038) and the NYUCI Center Support Grant, 9NIH/NCI 5 P30CA16087-310.

References

1. Victoria G, et al. Bone stimulation for fracture healing: What's all the fuss? Indian J Orthop. 2009; 43(2):117–20. [PubMed: 19838359]
2. Elsalanty ME, Genecov DG. Bone grafts in craniofacial surgery. Craniomaxillofac Trauma Reconstr. 2009; 2(3):125–34. [PubMed: 22110806]
3. Athanasiou VT, et al. Histological comparison of autograft, allograft-DBM, xenograft, and synthetic grafts in a trabecular bone defect: an experimental study in rabbits. Med Sci Monit. 2010; 16(1):BR24–31. [PubMed: 20037482]
4. Siddiqui NA, Owen JM. Clinical advances in bone regeneration. Curr Stem Cell Res Ther. 2013; 8(3):192–200. [PubMed: 23317467]
5. Mediero A, et al. Direct or indirect stimulation of adenosine A2A receptors enhances bone regeneration as well as bone morphogenetic protein-2. FASEB J. 2015; 29(4):1577–90. [PubMed: 25573752]
6. Fredholm BB, et al. International Union of Pharmacology. XXV. Nomenclature and classification of adenosine receptors. Pharmacol Rev. 2001; 53(4):527–52. [PubMed: 11734617]
7. He W, et al. Adenosine regulates bone metabolism via A1, A2A, and A2B receptors in bone marrow cells from normal humans and patients with multiple myeloma. FASEB J. 2013; 27(9):3446–54. [PubMed: 23682121]
8. Mediero A, et al. Brief Report: Methotrexate Prevents Wear Particle-Induced Inflammatory Osteolysis in Mice Via Activation of Adenosine A2A Receptor. Arthritis Rheumatol. 2015; 67(3): 849–55. [PubMed: 25533750]
9. Mediero A, Perez-Aso M, Cronstein BN. Activation of adenosine A(2A) receptor reduces osteoclast formation via PKA- and ERK1/2-mediated suppression of NFkappaB nuclear translocation. Br J Pharmacol. 2013; 169(6):1372–88. [PubMed: 23647065]
10. Mediero A, et al. Adenosine A2A receptor activation prevents wear particle-induced osteolysis. Sci Transl Med. 2012; 4(135):135ra65.
11. Mediero A, et al. Adenosine A(2A) receptor ligation inhibits osteoclast formation. Am J Pathol. 2012; 180(2):775–86. [PubMed: 22138579]

12. Montesinos MC, et al. Adenosine A(2A) receptor activation promotes wound neovascularization by stimulating angiogenesis and vasculogenesis. Am J Pathol. 2004; 164(6):1887–92. [PubMed: 15161625]
13. Coelho PG, Lemons JE. Physico/chemical characterization and in vivo evaluation of nanothickness bioceramic depositions on alumina-blasted/acid-etched Ti-6Al-4V implant surfaces. J Biomed Mater Res A. 2009; 90(2):351–61. [PubMed: 18508352]
14. LeGeros RZ. Properties of osteoconductive biomaterials: calcium phosphates. Clin Orthop Relat Res. 2002; (395):81–98. [PubMed: 11937868]
15. LeGeros RZ. Calcium phosphate-based osteoinductive materials. Chem Rev. 2008; 108(11):4742–53. [PubMed: 19006399]
16. Simon JL, et al. In vivo bone response to 3D periodic hydroxyapatite scaffolds assembled by direct ink writing. J Biomed Mater Res A. 2007; 83(3):747–58. [PubMed: 17559109]
17. Cai H. Application of 3D printing in orthopedics: status quo and opportunities in China. Ann Transl Med. 2015; 3(Suppl 1):S12. [PubMed: 26046057]
18. Rengier F, et al. 3D printing based on imaging data: review of medical applications. Int J Comput Assist Radiol Surg. 2010; 5(4):335–41. [PubMed: 20467825]
19. Szpalski C, et al. Bony engineering using time-release porous scaffolds to provide sustained growth factor delivery. J Craniofac Surg. 2012; 23(3):638–44. [PubMed: 22565873]
20. Simon JL, et al. MicroCT analysis of hydroxyapatite bone repair scaffolds created via three-dimensional printing for evaluating the effects of scaffold architecture on bone ingrowth. J Biomed Mater Res A. 2008; 85(2):371–7. [PubMed: 17688275]
21. Dutta Roy T, et al. Performance of hydroxyapatite bone repair scaffolds created via three-dimensional fabrication techniques. J Biomed Mater Res A. 2003; 67(4):1228–37. [PubMed: 14624509]
22. Sayama C, et al. Routine use of recombinant human bone morphogenetic protein-2 in posterior fusions of the pediatric spine and incidence of cancer. J Neurosurg Pediatr. 2015; 16(1):4–13. [PubMed: 25860984]
23. Cahill KS, McCormick PC, Levi AD. A comprehensive assessment of the risk of bone morphogenetic protein use in spinal fusion surgery and postoperative cancer diagnosis. J Neurosurg Spine. 2015; 23(1):86–93. [PubMed: 25860517]
24. Michna S, Wu W, Lewis JA. Concentrated hydroxyapatite inks for direct-write assembly of 3-D periodic scaffolds. Biomaterials. 2005; 26(28):5632–9. [PubMed: 15878368]
25. Silva NR, et al. Additive CAD/CAM process for dental prostheses. J Prosthodont. 2011; 20(2):93–6. [PubMed: 20561158]
26. Witek L, et al. Sintering effects on chemical and physical properties of bioactive ceramics. Journal of Advanced Ceramics. 2013; 2(3):274–284.
27. Goldman HM, Kindsvater J, Bromage TG. Correlative light and backscattered electron microscopy of bone--Part I: Specimen preparation methods. Scanning. 1999; 21(1):40–3. [PubMed: 10070782]
28. Mediero A, et al. Direct or indirect stimulation of adenosine A2A receptors enhances bone regeneration as well as bone morphogenetic protein-2. FASEB J. 2015
29. Singh K, et al. Clinical sequelae after rhBMP-2 use in a minimally invasive transforaminal lumbar interbody fusion. Spine J. 2013; 13(9):1118–25. [PubMed: 24029138]
30. Lam JY, et al. Safety and diagnostic accuracy of dipyridamole-thallium imaging in the elderly. J Am Coll Cardiol. 1988; 11(3):585–9. [PubMed: 3343462]
31. Lette J, et al. Safety of dipyridamole testing in 73,806 patients: the Multicenter Dipyridamole Safety Study. J Nucl Cardiol. 1995; 2(1):3–17. [PubMed: 9420757]
32. Fahim DK, et al. Routine use of recombinant human bone morphogenetic protein-2 in posterior fusions of the pediatric spine: safety profile and efficacy in the early postoperative period. Neurosurgery. 2010; 67(5):1195–204. discussion 1204. [PubMed: 20871458]
33. Mediero A, Cronstein BN. Adenosine and bone metabolism. Trends Endocrinol Metab. 2013; 24(6):290–300. [PubMed: 23499155]
34. TenHuisen KS, et al. Formation and properties of a synthetic bone composite: hydroxyapatite-collagen. J Biomed Mater Res. 1995; 29(7):803–10. [PubMed: 7593018]

35. Moreau JL, Weir MD, Xu HH. Self-setting collagen-calcium phosphate bone cement: mechanical and cellular properties. J Biomed Mater Res A. 2009; 91(2):605–13. [PubMed: 18985758]
36. Seitz H, et al. Three-dimensional printing of porous ceramic scaffolds for bone tissue engineering. J Biomed Mater Res B Appl Biomater. 2005; 74(2):782–8. [PubMed: 15981173]
37. Rabiee SM, Salimi-Kenari H, Solati-Hashjin M, Mortazavi SMJ. Study of biodegradable ceramic bone graft substitute. Advances in Applied Ceramics. 2008; 107(4):199–202. F.M.
38. Murphy SV, Atala A. 3D bioprinting of tissues and organs. Nat Biotechnol. 2014; 32(8):773–85. [PubMed: 25093879]
39. Klammert U, et al. 3D powder printed calcium phosphate implants for reconstruction of cranial and maxillofacial defects. J Craniomaxillofac Surg. 2010; 38(8):565–70. [PubMed: 20206538]
40. Klammert U, et al. Low temperature fabrication of magnesium phosphate cement scaffolds by 3D powder printing. J Mater Sci Mater Med. 2010; 21(11):2947–53. [PubMed: 20740307]
41. Inzana JA, et al. 3D printing of composite calcium phosphate and collagen scaffolds for bone regeneration. Biomaterials. 2014; 35(13):4026–34. [PubMed: 24529628]
42. Vorndran E, et al. Simultaneous Immobilization of Bioactives During 3D Powder Printing of Bioceramic Drug-Release Matrices. Advanced Functional Materials. 2010; 20(10):1585–1591.

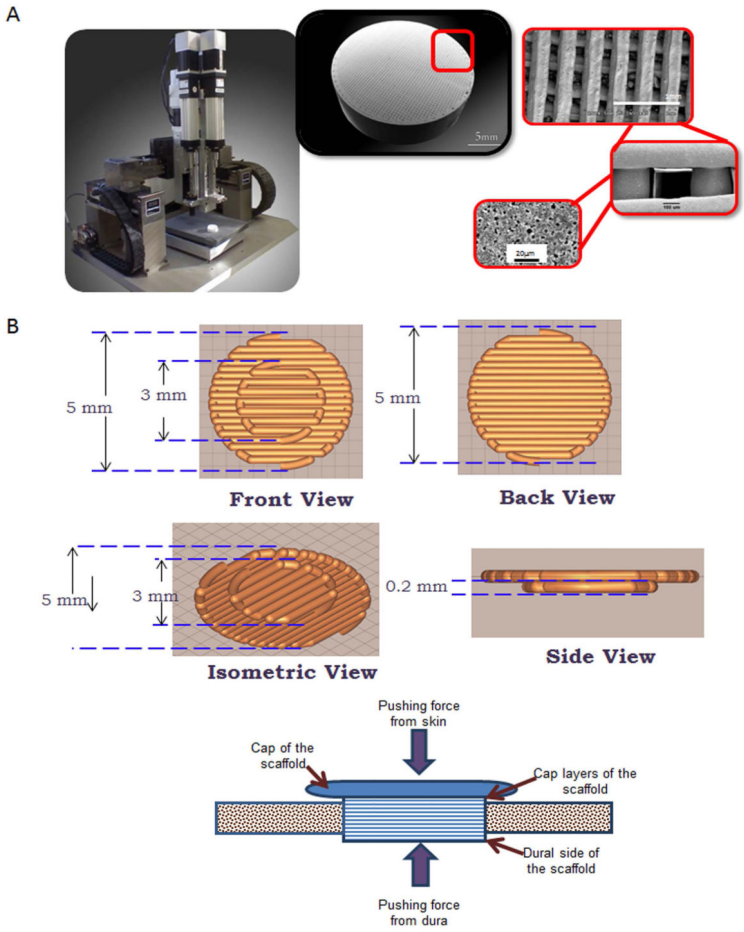

Figure 1. Scaffolds used for implantantation into calvarial defects

A) 3-D Robocast Printer used to fabricate scaffolds. B) Shown are digital images of ceramic scaffolds used to fill trephine defects in mice

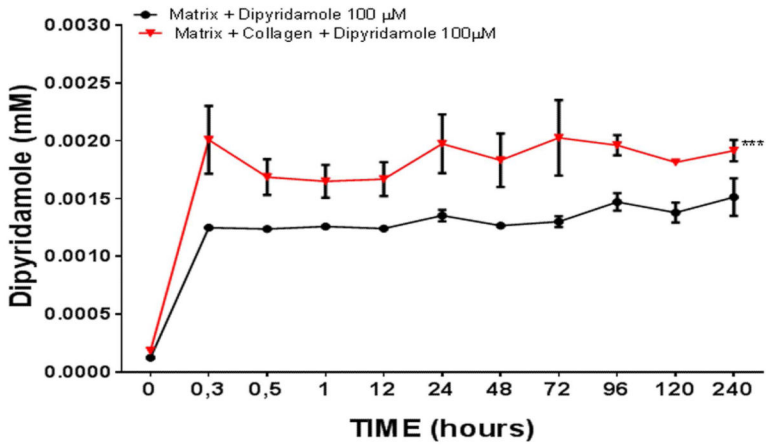

Figure 2. Dipyridamole release from scaffolds

Scaffolds were coated with bovine collagen and then immersed in a solution of dipyridamole (100µM). The coated scaffolds were then immersed in 0.5ml of saline - and the concentration of dipyridamole quantitated as A_{405} at the time points indicated in methods (n=5 each time point). Each determination was carried out in triplicate and results are shown as mean (±SEM). *** $p<0.001$ collagen coated scaffolds vs non coated scaffolds, two-way ANOVA and Bonferroni post-hoc tes.

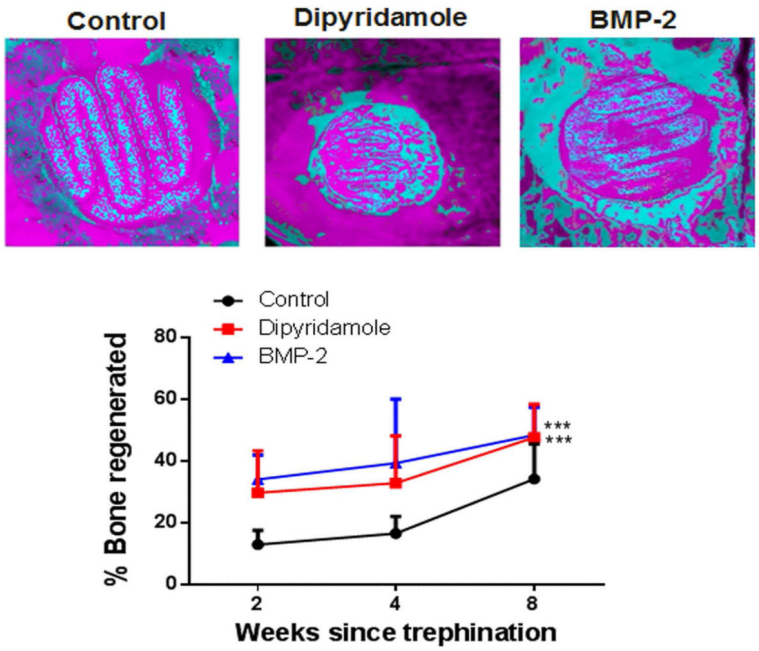

Figure 3. Dipyridamole and BMP2 promote bone growth on a βTCP/HA scaffold

Scaffolds coated with bovine collagen alone were immersed in saline, BMP2 or dipyridamole and implanted into trephine defects in mouse calvaria, A). Representative microCTs of scaffolds in trephine defects after 8 weeks, blue is new bone density, red is scaffold and old bone. B). Quantitation of microCT- in each treatment group after 2, 4 or 8 weeks following implantation. Shown are means (±SEM) from 5 different animals per group. 2-way ANOVA demonstrates that both dipyridamole- and BMP2-coated scaffolds promote greater bone regeneration than control scaffolds. *** $p<0.001$ dipyridamole and BMP-2 coated scaffolds vs control scaffolds, two-way ANOVA and Bonferroni post-hoc tes.

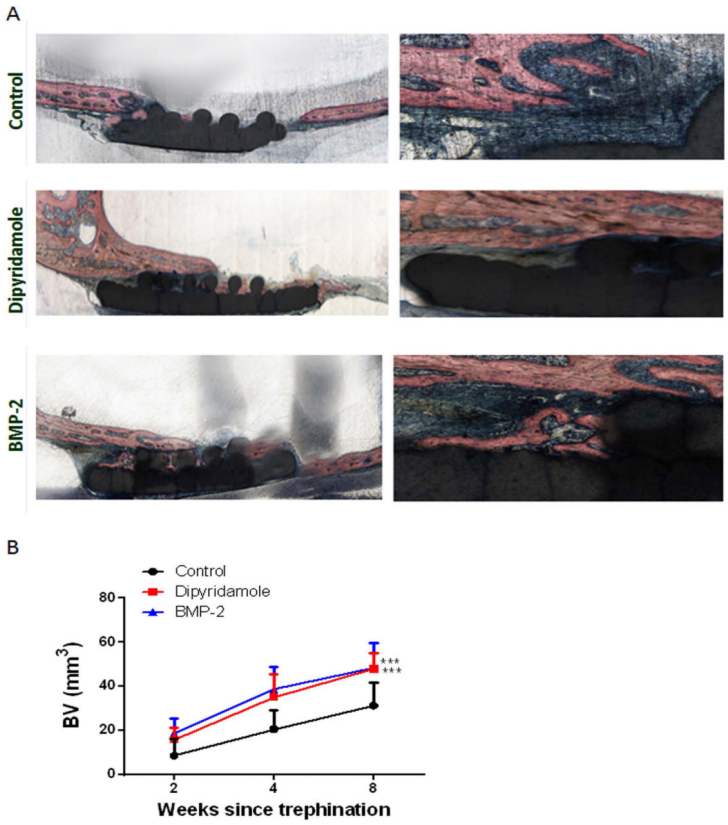

Figure 4. Dipyridamole and BMP2 promote bone growth on a βTCP/HA scaffold

Scaffolds coated with bovine collagen alone were immersed in saline, BMP2 or dipyridamole, and implanted into trephine defects in mouse calvaria, A) Representative histologic sections of scaffolds in trephine defects after 8 weeks, blue is new bone density, red is scaffold and old bone. Sections were embedded in methyl methacrylate and, after cutting and polishing, were stained with Stevenel's Blue and von Giessen stain (Bone is pink). Original Magnification 20X and 40X. B) Quantitation of bone regeneration in each treatment group after 2, 4 or 8 weeks following implantation. Shown are means (±SEM) from 5 different animals per group. 2-way ANOVA demonstrates that both dipyridamole- and BMP2-coated scaffolds promote greater bone regeneration than control scaffolds. *** $p<0.001$ dipyridamole and BMP-2 coated scaffolds vs control scaffolds, two-way ANOVA and Bonferroni post-hoc test.

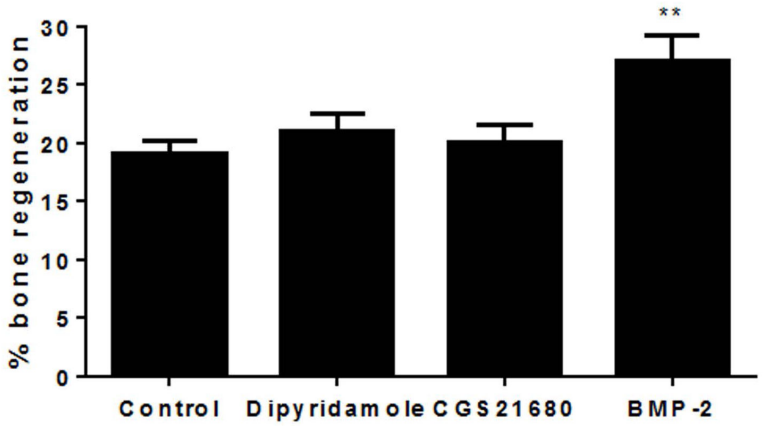

Figure 5. Neither dipyridamole nor the A2AR agonist CGS21680 increases bone formation on ceramic scaffolds in A2AR knockout mice

Trephination and implantation of ceramic scaffolds coated with collagen immersed in BMP-2, dipyridamole (100μM), CGS21680 (100μM) or saline were carried out in mice lacking A2AR. Mice were sacrificed 4 weeks later, and new bone and matrix were quantified by microCT. There is significantly greater new bone formation with the BMP2-treated scaffolds but not with dipyridamole-, CGS-21680-, or saline-treated scaffolds. Each bar represents the mean (±SEM) of results from 5 mice for each group. **p<0.01 vs control scaffold, one-way ANOVA and Bonferroni post-hoc test..